Available online at www.sciencedirect.com
SCIENCE DIRECT®
Biomaterials 25 (2004) 3177–3185
Biomaterials
www.elsevier.com/locate/biomaterials

Activity of plasma sprayed yttria stabilized zirconia reinforced hydroxyapatite/Ti–6Al–4V composite coatings in simulated body fluid

Y.W. Gu[a], K.A. Khor[a,*], D. Pan[b], P. Cheang[c]

[a] School of Mechanical & Production Engineering, Nanyang Technological University, 50, Nanyang Avenue, Singapore 639798, Singapore
[b] Singapore Institute of Manufacturing Technology, 71 Nanyang Drive, Singapore 638075, Singapore
[c] School of Materials Engineering, Nanyang Technological University, 50, Nanyang Avenue, Singapore 639798, Singapore

Received 20 February 2002; accepted 23 September 2003

Abstract

Hydroxyapatite (HA)/yttria stabilized zirconia/Ti–6Al–4V bio-composite coatings deposited onto Ti–6Al–4V substrate through a plasma spray technique were immersed in simulated body fluid (SBF) to investigate their behavior in vitro. Surface morphologies and structural changes in the coatings were analyzed by scanning electron microscopy, thin-film X-ray diffractometer, and X-ray photoelectron spectroscopy. The tensile bond strength of the coatings after immersion was also conducted through the ASTM C-633 standard for thermal sprayed coatings. Results showed that carbonate-containing hydroxyapatite (CHA) layer formed on the surface of composite coatings after 4 weeks immersion in SBF solution, indicating the composite coating possessed excellent bioactivity. The mechanical properties were found to decrease with immersion duration of maximum 56 days. However, minimal variation in mechanical properties was found subsequent to achieving supersaturation of the calcium ions, which was attained with the precipitation of the calcium phosphate layers. The mechanical properties of the composite coating were found to be significantly higher than those of pure HA coatings even after immersion in the SBF solution, indicating the enhanced mechanical properties of the composite coatings.

Keywords: Biomaterials; Simulated body fluid; Hydroxyapatite; Composite coating; Plasma spraying

1. Introduction

Synthetically produced hydroxyapatite (HA) has similar crystallographic structure as the apatite crystallites found in living bone tissues [1,2]. It has received increasing attention as a bone implant material to promote accelerated fixation of orthopaedic prostheses [3]. However, sintered HA has been reported to be susceptible to fatigue failure, which imposed an acute restriction to the applied load in many clinical applications [4]. The problem can be solved through applying HA coatings onto metal substrates [5]. In this arrangement, the biocompatibility of implants is assured by the presence of HA while the mechanical properties are supplemented by the metal substrate.

In recent years, it has been recognized that the mechanical stability of the interface between the HA coating and titanium alloy substrate could be an impediment either during surgical operation or after implantation, due to the brittle nature of HA and the uncertain long-term integrity of the interface [6,7]. HA-based composites that are reinforced with bioinert ceramics or metals in the form of powders, or fibers have attracted much attention. Ti–6Al–4V is a mechanically strong and biocompatible metal alloy. Previous studies on HA/Ti–6Al–4V composite coating showed that its mechanical properties are undoubtedly superior to that of pure HA coating, while maintaining good bioactivity following immersion in SBF [8,9]. Yttria stabilized zirconia (YSZ) is often used as reinforcement for many ceramics because it has the merits of high strength and enhanced toughening characteristics during crack–particle interactions [10]. Biocompatibility is another crucial merit of YSZ [11]. Reports on plasma

*Corresponding author. Tel.: +65-67905526; fax: +65-6791-1859.
E-mail address: mkakhor@ntu.edu.sg (K.A. Khor).

0142-9612/$ - see front matter © 2003 Elsevier Ltd. All rights reserved.
doi:10.1016/j.biomaterials.2003.09.101

sprayed HA/YSZ coatings revealed that the addition of YSZ to HA produced better mechanical properties than those of the bulk HA alone [12,13].

Bioactive materials bond to living bone through a collagen-free apatite layer which is formed on their surface. The thickness and crystal size of the apatite are dependent on the salient characteristics of the bioactive material such as chemical composition and surface integrity [14]. This apatite layer can also be produced in vitro using the SBF since SBF has almost the same ion concentrations as those of the human blood plasma [15]. Thus, the in vitro tests may be used as a criterion to assess the in vivo bioactivity. Previous work showed that the rapid surface dissolution and bone-like apatite layer formation occurred for plasma sprayed HA coatings after immersion in SBF [16,17].

To bridge the gap in plasma sprayed HA coatings having low bond strength, HA/YSZ/Ti–6Al–4V composite coatings were developed in this study. A novel approach of ceramic slurry mixing was used to prepare composite powders with an inner core of Ti–6Al–4V swathed by a layer of mixed HA/YSZ powders. These composite powders were employed as feedstock for subsequent preparation of HA/YSZ/Ti–6Al–4V composite coatings by plasma spray technique [21]. The composite coatings prepared by the composite powders were designed to improve the mechanical stability of the coating when exposing the coating to the simulated body fluid (SBF). In this paper, the bioactivity and mechanical stability of the composite coating were studied by immersing the coatings in SBF. Microstructure and phase composition of HA/YSZ/Ti–6Al–4V composite coatings were characterized with scanning electron microscopy (SEM) and thin-film X-ray diffractometer (TF-XRD) techniques, respectively. Microhardness, Young's modulus and tensile bond strength of the composite coatings were also evaluated. The chemical composition of the apatite layer formed on the surface of the composite coating was determined by X-ray photoelectron spectroscopy (XPS) analysis. The dissolution characteristics of pure HA coatings and HA/Ti–6Al–4V composite coatings were used for comparison in this study.

2. Experimental materials and procedure

HA 35 wt%/YSZ 15 wt%/Ti–6Al–4V 50 wt% composite powders were prepared by novel ceramic slurry mixing method [8]. The binder was formed when polyvinyl alcohol (PVA), 20% by weight, was mixed with 100 ml distilled water. The spherical HA powders with a particle size smaller than 20 μm and the angular YSZ powders with a particle size smaller than 5 μm were poured into the binder, with constant stirring, for 5 h to form the slurry, by means of a mechanical stirrer. The angular Ti–6Al–4V powders with the particle size range of 45–105 μm were then added into the HA/YSZ slurry and stirred for another 5 h. The HA/YSZ coated Ti–6Al–4V powders were debound at 450°C for 1 h and further consolidated at 600°C for 6 h in vacuum with a vacuum level of 5 Pa.

The titanium plates with a dimension of $50 \times 40 \times 3\,mm^3$ were used for the deposition of the coatings. The substrate was sandblasted with Al_2O_3 grit of average 600 μm and it was subsequently cleaned ultrasonically using acetone. Prior to deposition of the composite coatings, the substrate was preheated in order to reduce the residual thermal stresses in the coating. A robot-controlled, fully computerized 100 kW direct current (dc) plasma torch (SG-100 Praxair Thermal Inc., USA) equipped with an advanced computerized closed-loop powder feeder system was used for the deposition of HA/YSZ/Ti–6Al–4V composite coatings onto Ti–6Al–4V substrates. Table 1 lists the plasma spraying parameters during the deposition. The thickness of the coating after plasma spraying was in the range 200–250 μm.

The plasma sprayed Ti–6Al–4V plate was cut into small pieces with dimensions of $15 \times 15 \times 3\,mm^3$. The samples were suspended in vials containing 50 ml SBF using Nylon strings to study their in vitro behavior. The SBF was prepared using Kokubo's formulation [18]. The ion concentrations in SBF were similar to those of the human blood plasma, as shown in Table 2. The solution was buffered to a physiological pH of 7.25 at 37°C with tris(hydroxymethyl)-aminomethane and hydrochloric acid (HCl). The composite coatings were

Table 1
Plasma spraying parameters

Primary gas	Argon (1.85 m^3/h)
Auxiliary gas	Helium (1.64 m^3/h)
Carrier gas	Argon (0.30 m^3/h)
Net energy	12 kW
Standoff distance	8.5 cm
Powder feedrate	10 g/min; 3.5 rpm
Gun transverse speed	250 mm/s

Table 2
Ion concentration of SBF in comparison with human blood plasma

Species	Ion concentration (mmol/l)	
	Blood plasma	SBF
Ca^{2+}	2.5	2.2
HPO_4^{2-}	1.0	0.8
Na^+	142.0	140.3
Cl^-	148.8	148.0
Mg^{2+}	1.5	1.3
K^+	5.0	5.3
SO_4^{2-}	0.5	0.5
HCO_3^-	4.2	4.0

immersed in SBF for various periods of 1, 7, 14, 28 and 56 days. The solution was agitated daily to help maintain uniform ion concentrations. After pre-determined time periods of immersion, the samples were taken out, gently rinsed with distilled water and dried at room temperature. The experiment was performed at 37°C in a temperature-controlled water bath.

The phase composition of the composite coatings, after immersion in SBF for various periods, was determined with Shimadzu 6000 XRD using CuKα radiation at 40 kV and 30 mA. The chemical composition of the apatite layer formed on the surface was analyzed by XPS. The surface morphology of the composite coatings was analyzed through JEOL JSM-5600LV SEM equipped with energy dispersive X-ray spectrometry (EDX). The calcium (Ca^{2+}) concentration in the solutions was measured directly after the samples were removed, using Perkin-Elmer Plasma 400 inductively coupled plasma atomic emission spectrometer (ICP-AES).

The Knoop indenter was used to determine the Young's modulus E as follows [19,20]:

$$\frac{b'}{a'} = \frac{b}{a} - \frac{\alpha H_k}{E}, \quad (1)$$

where H_k denotes the Knoop microhardness; b'/a' denotes the ratio of the short (b') and long (a') indention diagonals after elastic recovery; b/a is the ratio of the known Knoop indenter geometry (1/7.11); α is a constant, having a value of 0.45. A minimum sample size of 10 was adopted to evaluate H_k and E values.

The bond strength of HA/YSZ/Ti–6Al–4V composite coatings after immersion was evaluated using standard tensile adhesion test (ASTM-C633) for thermal sprayed coatings. Two identical cylindrical Ti–6Al–4V stubs were used as a set, one with the coating on the surface and the other without. A high performance DP-460 Epoxy Adhesive (3M, USA) with a maximum bond strength of 40 MPa was used to join the two stubs. The surface of the uncoated stub was sand blasted to enhance the adhesion strength. The bond strength was measured using an Instron 4302 tester at a crosshead speed of 1 mm min^{-1}. Five specimens were tested and an average was obtained for each time period.

3. Results and discussion

The morphology of HA and YSZ coated Ti–6Al–4V composite powders prepared by the ceramic slurry mixing approach is shown in Fig. 1. Ti–6Al–4V powders are uniformly coated by HA and YSZ powders. By using the composite powders for plasma spraying, the oxidation of Ti–6Al–4V could be effectively curtailed, and the chemical homogeneity of the coating could be significantly improved [8]. Fig. 2 shows the cross-section

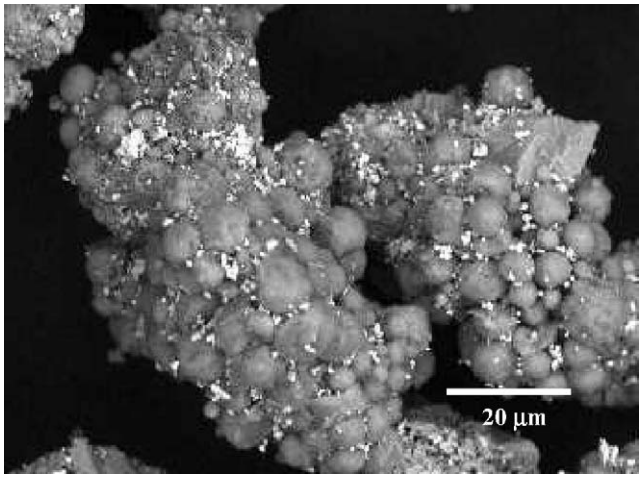

Fig. 1. Morphology of HA/YSZ/Ti–6Al–4V composite powders (small white particles are YSZ and the gray spherical particles are HA).

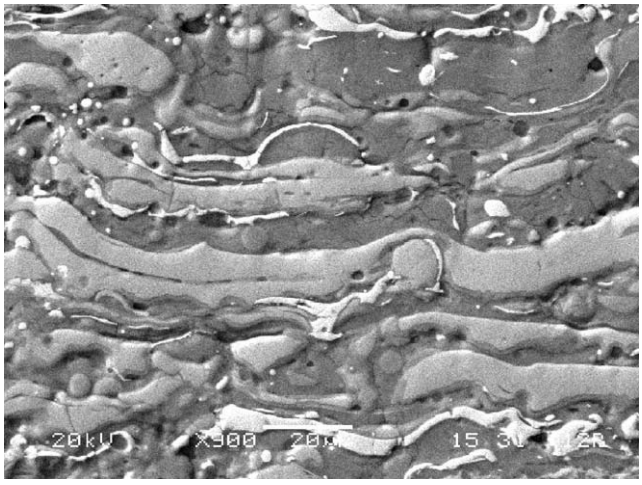

Fig. 2. Cross-section microstructure of HA/YSZ/Ti–6Al–4V composite coating.

microstructure of HA/YSZ/Ti–6Al–4V composite coating. The light gray area is Ti alloy and the dark gray area is HA. YSZ is evident by the presence of white strips and small white specks within HA and Ti alloy.

3.1. Phase and chemical compositions

Fig. 3 shows the XRD patterns of HA/YSZ/Ti–6Al–4V composite coatings before and after immersion in SBF for various periods. Ti, ZrO_2, HA and amorphous calcium phosphate are the main phases in the plasma sprayed composite coating before immersion in SBF. The diffractogram of the as-sprayed composite coating also shows traces of α-TCP and CaO phases. The appearance of the trace compounds of α-TCP and CaO in the plasma sprayed HA coatings has also been reported in some papers [21]. CaO peak is also observed for HA/Ti–6Al–4V coatings after plasma spraying, as

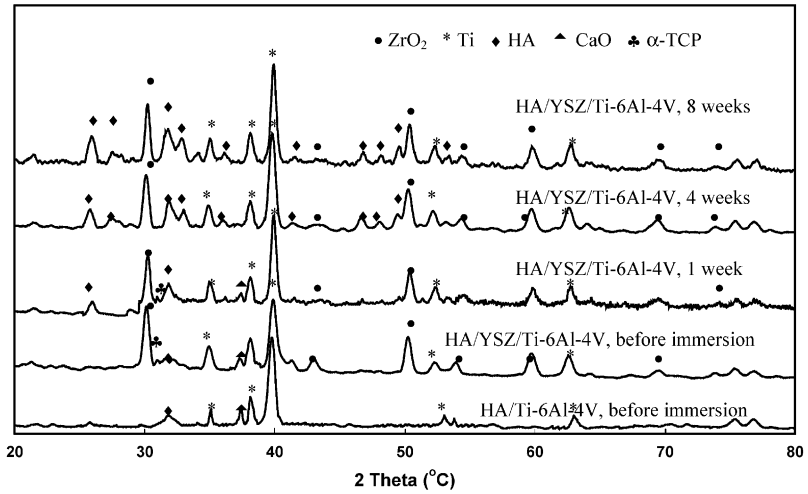

Fig. 3. XRD patterns of HA/YSZ/Ti–6Al–4V composite coatings as a function of immersion time in SBF.

shown in Fig. 3. CaO and TCP phases are formed as a result of the high temperature of plasma spray, during which a small portion of HA is thermally decomposed. With an increase in the immersion period in SBF, the intensities of α-TCP and CaO decrease. After immersion the coating in SBF for 1 week, α-TCP phase disappears completely. The CaO peak also disappears from the XRD pattern after immersion in SBF for 4 weeks. Following 4 weeks of immersion henceforth, the XRD pattern only shows diffraction peaks of HA, ZrO_2 and Ti, indicating that α-TCP and CaO phases are dissolved in the solution. This can be explained in terms of the reaction of α-TCP and CaO with water and their respective dissolution in water. When the composite coating is immersed into SBF, α-TCP and CaO phases react with water molecules according to the following reactions [22]:

$$4Ca_3(PO_4)_2 + H_2O \rightarrow Ca_{10}(PO_4)_6(OH)_2 + 2Ca^{2+} + 2HPO_4^{2-}, \quad (2)$$

$$CaO + H_2O \rightarrow Ca^{2+} + 2OH^-. \quad (3)$$

The XRD patterns record a noticeable increase in HA content after soaking the composite coatings in SBF. The X-ray diffraction intensity of HA intensifies with increasing immersion duration. The dissolution of the metastable components occurs at the initial stage of immersion, releasing calcium and phosphorus ions into the solution. This in turns increases the supersaturation of the solution, and precipitation of the apatite onto the surface of coatings occurs by consuming the calcium and phosphorus ions in the SBF. For example, according to Eq. (2), α-TCP reacts with water molecules, forming a crystalline apatite structure. This is in agreement with the observation by Groot et al. who found that the crystallinity of the coatings increased when coatings were kept in aqueous solutions for several weeks [23]. Fig. 3 revealed that the diffraction peak of the (0 0 2) crystal plane is much more pronounced than that of similar crystal plane of HA in the standard PDF card. This suggests that the apatite formed on the surface of the composite coatings have a preference along the crystal orientation of [0 0 1].

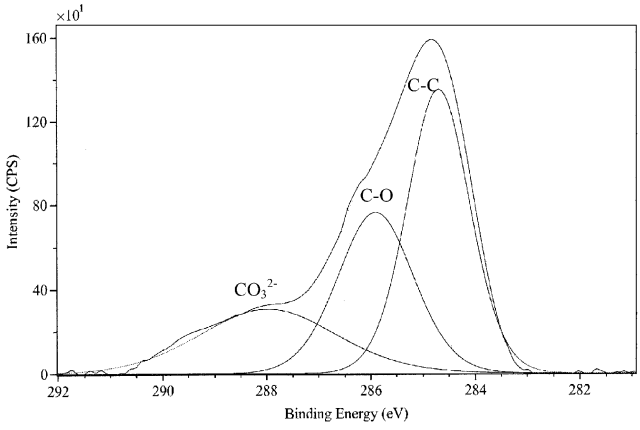

Fig. 4. XPS C 1s spectrum of HA/YSZ/Ti–6Al–4V composite coating.

The precipitation that formed on the surface of the composite coatings was examined by XPS. XPS analysis on the surface layer shows the presence of C, Ca, P and O. The XPS C1s spectrum that consists of three peaks is shown in Fig. 4. The peak at 284.5 eV and the peak at 285.5 eV correspond to C–C and C–O peaks, respectively, which exist on the surface layer due to the carbon contamination. The C1s peak at 287.8 eV is carbonated group CO_3^{2-} [14], revealing that the surface layer of the coating after immersion in SBF is carbonate containing.

3.2. Surface morphology examination

The surface morphologies of the HA/YSZ/Ti–6Al–4V coatings before and after immersion in SBF for various

periods are shown in Fig. 5. Initially, the surface is covered by well-molten (smooth) splats and the fine microcracks as shown in Fig. 5a. After 1 day of immersion, the top surface layer of the coatings appeared distinctly dissolved during immersion; more microcracks seems to have appeared on the surface of the coatings (Fig. 5b). The dissolved layer may expose microcracks already present within the coatings or may propagate the existing surface cracks due to internal thermal residual stresses being released. The crack size and crack density increase with immersion duration, suggesting a dissolution process. Cracked regions in the coating and delaminated segments can also be observed from Fig. 5b. The other calcium phosphate phases, e.g., α-TCP and CaO, have a high resorbability and can aid in the dissolution of the coating and fragmentation of plasma sprayed lamellae. After 1 week of immersion, multiple large cracks that propagate along the whole surface of the coating can be observed. After 2 weeks, small spherical particles with diameter 2–5 μm were found throughout the composite coating surface. This was consistent with the results obtained from the in vitro study of HA/Ti–6Al–4V coatings. On the HA/Ti–6Al–4V coatings, the surface was covered with a newly formed layer consisting of small granular precipitates after 2-week soaking [9]. Similar apatite spherulites were observed by other researchers after immersion of the HA coatings in SBF [24,25]. Such SEM observation supports the XRD results that the apatite peaks keep raising after immersion. Higher magnification surface morphology of the composite coating showed many pores on the surface, which was apparently formed as a consequence of dissolution. Cracks formed through shrinkage upon drying appear in the apatite layer [26]. These cracks were apparently caused by stress relief during dehydration, and will not appear in the real body environment due to the characteristics of the moist environment. EDX analysis on the surface layer of the coatings with different immersion durations shows the presence of C, O, Ca and P. This is in consistent with the XPS results, which show the same elements on the surface of the coating after immersion. The above results clearly showed that the surface layer formed on the composite coatings demonstrate that the layer formed on the sample surface was carbonate-containing apatite.

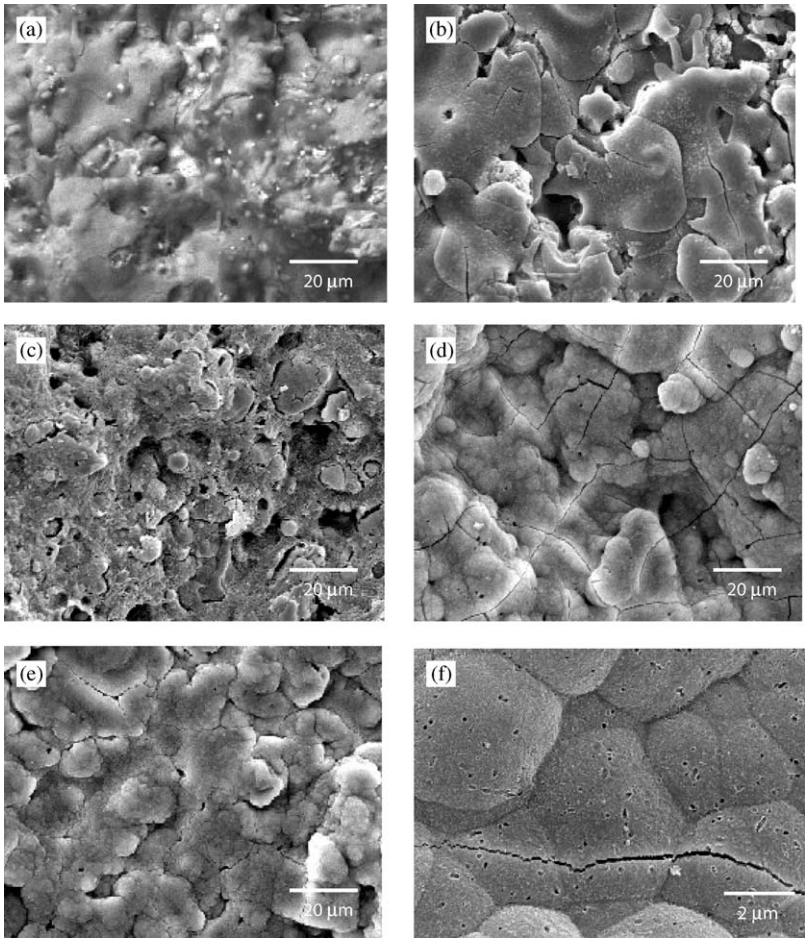

Fig. 5. Surface morphologies of HA/YSZ/Ti–6Al–4V composite coatings after soaking in SBF for various periods of time: (a) before soaking; (b) 1 day; (c) 3 days; (d) 1 week; (e) 4 weeks; and (f) high magnification of (e).

Apatite-forming ability is a very important surface reaction property in forming a chemical bond between bony tissue and bioactive materials. The observation in this study evidences that the apatite layer can be formed on the surface of the plasma sprayed composite coatings. This shows the excellent bioactivity of the HA/YSZ/Ti–6Al–4V composite coatings, which have the ability to induce bone-like apatite nucleation and growth on its surface from a metastable calcium phosphate solution. Therefore, it can be expected that the chemical bond can be formed between the composite coating and the bony tissue after implantation.

3.3. Element concentration analysis

Fig. 6 shows the ICP chemical analysis of the calcium ion concentrations in the SBF for pure HA coatings [27], HA/Ti–6Al–4V composite coatings and HA/YSZ/Ti–6Al–4V composite coatings for 1 day, 1, 2, 4 and 8 weeks. The calcium ion concentrations of the three types of coatings exhibit similar trends with the immersion periods in SBF. The calcium ion concentration in the solution increases rapidly in the initial 2 weeks of immersion. By considering the XRD results, it can be concluded that the increase in the calcium concentration is mainly due to the dissolution of CaO and TCP phases in the as-sprayed coatings. Thereafter, the dissolution rate decreases and the calcium ion concentration starts to decrease, indicating a continuous precipitation of the bone-like apatite layer. The nucleation and growth of the apatite consume calcium and phosphorus in the solution. Thus, the amount of the calcium concentration reduces. After 2 weeks of immersion, the depletion of Ca is obvious, indicating that the nucleation of the apatite has been very active during the first 2 weeks. It can be observed from Fig. 6 that there is a significant difference

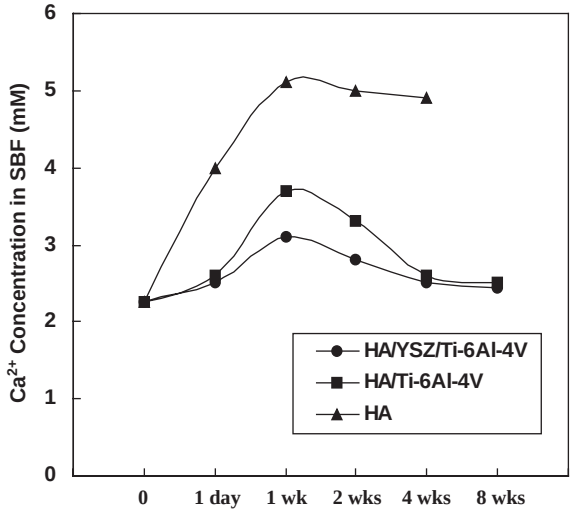

Fig. 6. ICP analysis of variation of calcium concentrations as a function of immersion time in SBF [9,27].

in the dissolution rate for the three types of coatings. The dissolution rate for pure HA coatings is undeniably the highest. The kinetics of dissolution is the most moderate for HA/YSZ/Ti–6Al–4V composite coatings, whereas, the dissolution of the plasma sprayed HA/Ti–6Al–4V composite coatings lies between the two aforementioned material coating systems. This is probably due to the fact that there is less HA in the composite coatings. Furthermore, ZrO_2 and Ti phases do not dissolve in the SBF and the existence of Ti–6Al–4V reduces the porosity in the composite coating [8], which in turn decreases the dissolution phenomenon. Since HA becomes more soluble as more OH^- ions are lost [28], the relatively slower dissolution rate for the composite coatings can also be explained by their ability to preserve OH^- ions during plasma spraying [27].

It has been demonstrated from SEM/EDX, XRD and XPS analyses that a layer of bone-like carbonate containing apatite can be formed on the surface of the HA/YSZ/Ti–6Al–4V composite coatings. The ICP result further proves that the increase in the concentration of calcium ions in the solution induces the formation of apatite layer on the coating. The increase in the ion concentrations increases the apatite ionic activity product (IP). The constituent ions that formed the apatite are shown in the following equation:

$$10Ca^{2+}+6PO_4^{3-}+2OH^- \rightleftharpoons Ca_{10}(PO_4)_6(OH)_2. \quad (4)$$

The IP of the apatite in an aqueous solution is given by the following equation [29]:

$$IP = (\alpha_{Ca^{2+}})^{10}(\alpha_{PO_4^{3-}})^6(\alpha_{OH^-})^2 = (\gamma_{Ca^{2+}})^{10}(\gamma_{PO_4^{3-}})^6(\gamma_{OH^-})^2[Ca^{2+}]^{10}[PO_4^{3-}]^6[OH^-]^2, \quad (5)$$

where α and γ are the activity and the activity coefficient, respectively. Square bracket is the ionic concentration.

The relative supersaturation, σ, can be expressed by the following equation [30]:

$$\sigma = \frac{IP^{1/v} - K^{1/v}}{K^{1/v}} = \frac{IP^{1/v}}{K} - 1, \quad (6)$$

where K is the solubility product. v is the number of ions in the molecule which is 18 for apatite.

From Eqs. (5) and (6), it can be concluded that the degree of supersaturation increases with an increase in the ion concentration in the SBF. In the initial 2-week immersion in SBF, the calcium and phosphate ions released from the composite coating increase the degree of supersaturation of the SBF. This will decrease the free energy for the formation of an embryo with critical size, which is favorable for the nucleation and growth of the apatite. The higher the degree of supersaturation, the higher the nucleation rate and quantity of the apatite on the surface of the composite coatings, as revealed in Figs. 5 and 6. In the body environment, two types of calcium phosphates could be formed. One is dicalcium phosphate $CaHPO_4 \cdot 2H_2O$ (C_2P) which is stable at

pH < 4.2, and the other is HA which is a stable phase at pH > 4.2. The pH value of the SBF in the present work is 7.4. Therefore, HA is formed on the surface of the composite coatings. Once the apatite nuclei are formed, they grow spontaneously by consuming the calcium, phosphate and carboxyl ions from the surrounding SBF. After 2-week immersion of the composite coatings in SBF, there is a decrease in the ion concentration due to the precipitation of the apatite.

3.4. Hardness, Young's modulus and bond strength

The variation of Knoop hardness, Young's modulus and tensile bond strength of HA/YSZ/Ti–6Al–4V composite coatings with the SBF immersion duration is shown in Figs. 7–9, respectively. The values of mechanical properties of pure HA coatings [16] and HA/Ti–6Al–4V composite coatings [9] are also shown in Figs. 7–9 for comparison. It can be observed that the mechanical properties values of HA/YSZ/Ti–6Al–4V and HA/Ti–6Al–4V composite coatings are much higher than those of the HA coatings before immersion. This is due to the fact that YSZ has the attributes of high strength and stress-induced phase transformation toughening, and Ti–6Al–4V is a metallic and ductile material. With the addition of YSZ and Ti–6Al–4V, the brittle nature of HA can be significantly improved. Therefore, high mechanical properties for the composite coatings are expected.

The mechanical properties are found to decrease with increasing immersion periods. A distinct drop in mechanical properties during the first 4 weeks is recorded. After 4 weeks of immersion, only slight degradation in mechanical properties for composite coatings can be observed. The degradation of mechanical properties following immersion in SBF comes mostly from the continuation of chemical dissolution of coatings. The dissolution process weakens the interlamellar microstructure in the coating and the bonding of the interface between coating and substrate. The coatings seem to reach a steady stage with a mild change in mechanical properties with the immersion time after 4-week immersion, which is due to the saturation of ion concentration in SBF.

Among the three types of coatings shown in Figs. 7–9, HA coating has been found to dissolve the fastest, which results in more bonding decay at the interface of coating and substrate. Consequently, the mechanical properties have been found to decrease proportionally. The HA/YSZ/Ti–6Al–4V coating exhibits the slowest dissolution rate. Therefore, the reduction in mechanical properties of HA/YSZ/Ti–6Al–4V composite coating as a function

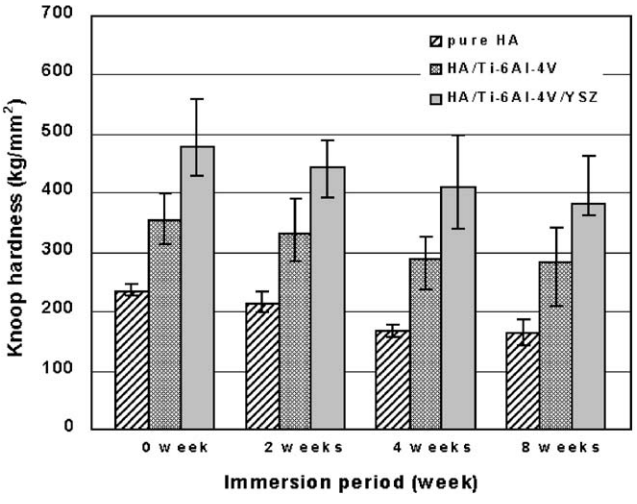

Fig. 7. Knoop hardness of composite coatings after immersion in SBF.

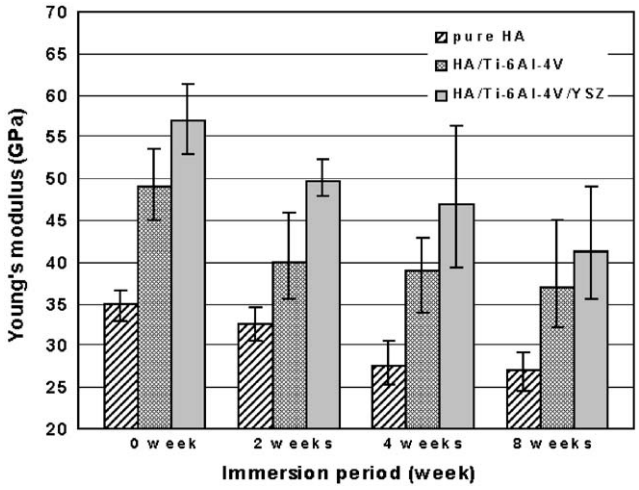

Fig. 8. Young's modulus of composite coatings after immersion in SBF.

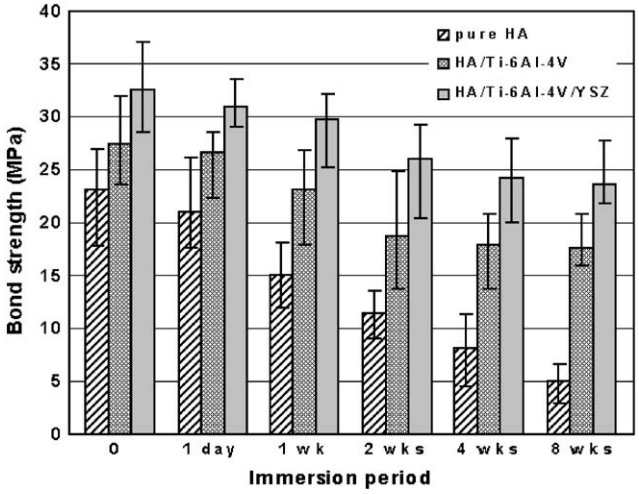

Fig. 9. Bond strength of composite coatings after immersion in SBF.

of immersion duration is significantly mitigated than that of the HA coating.

The fracture surface of the coatings after tensile bond strength test shows a mixed mode failure of cohesive and adhesive failure. Cohesive failure is more commonly found in the high strength coatings. The improved bond strength values of the composite coatings suggests a much better interface bonding between the lamellae and the coating/substrate compared with pure HA coatings.

4. Conclusions

The dissolution behavior in simulated body fluid (SBF) and the tensile adhesion strength degradation of plasma sprayed hydroxyapatitite (HA)/yttria stabilized zirconia (YSZ)/Ti–6Al–4V composite coatings were studied. The coatings were found to undergo two bio-integration processes, i.e., dissolution and the subsequent precipitation of apatite phase. Morphological and phase analyses showed that the dissolution rate of HA/YSZ/Ti–6Al–4V composite coating was significantly slower than that of the 100% HA coating. The calcium ion concentration in SBF confirmed this argument, where the increase in concentration was approximately 0.13 mM per day for the first 7 days in the HA/YSZ/Ti–6Al–4V composite coating, while in the HA coating, the corresponding rate of increase was 0.43 mM per day. Coatings were found to degrade correspondingly with the immersion time. However, the mechanical properties of HA/YSZ/Ti–6Al–4V composite coatings was found to be much superior to those of pure HA coatings following immersion in SBF. The tensile adhesion strength of the HA/YSZ/Ti–6Al–4V composite coating reduced by $\sim$27.7% after 4 weeks in the SBF, while the decrease in the HA coating was found to be $\sim$78.8% over the same period.

References

[1] Suchanek W, Yoshimura M. Processing and properties of hydroxyapatite-based biomaterials for use as hard tissue replacement implants. J Mater Res 1998;13:94–117.

[2] Willmann G. Coating of implants with hydroxyapatite material connections between bone and metal. Adv Eng Mater 1999;1(2):95–105.

[3] MacDonald DE, Betts F, Stranick M, Doty S, Boskey AL. Physicochemical study of plasma-sprayed hydroxyapatite-coated implants in humans. J Biomed Mater Res 2001;54(4):480–90.

[4] Hench LL. Bioceramics. J Am Ceram Soc 1998;81:1705–28.

[5] Lynn AK, DuQuesnay DL. Hydroxyapatite-coated Ti–6Al–4V Part 1: the effect of coating thickness on mechanical fatigue behavior. Biomaterials 2002;23(9):1937–46.

[6] Zheng XB, Huang MH, Ding CX. Bond strength of plasma-sprayed hydroxyapatite/Ti composite coatings. Biomaterials 2000;21(8):841–9.

[7] Simmons CA, Valiquette N, Pilliar RM. Osseointegration of sintered porous-surfaced and plasma spray-coated implants: an animal model study of early post implantation healing response and mechanical stability. J Biomed Mater Res 1999;47(2):127–38.

[8] Khor KA, Gu YW, Quek CH, Cheang P. Plasma spraying of functionally graded hydroxyapatite/Ti–6Al–4V coatings. Surf Coat Technol 2003;168(2–3):195–201.

[9] Gu YW, Khor KA, Cheang P. In vitro studies of plasma sprayed hydroxyapatite/Ti–6Al–4V composite coatings. Biomaterials 2003;24(9):1603–11.

[10] Chou BY, Chang E, Yao SY, Chen JM. Phase transformation during plasma spraying of hydroxyapatite–10-wt%-zirconia composite coating. J Am Ceram Soc 2002;85(3):661–9.

[11] Hulbert SF. In: Hench LL, Wilson J, editors. The use of alumina and zirconia in surgical implants. An introduction to bioceramics. Singapore: Word Scientific Publishing Co.; 1993. p. 25–40.

[12] Chou BY, Chang E. Plasma-sprayed hydroxyapatite coating on titanium alloy with ZrO_2 second phase and ZrO_2 intermediate layer. Surf Coat Technol 2002;153(1):84–92.

[13] Fu L, Khor KA, Lim JP. Effects of yttria stabilized zirconia on plasma sprayed hydroxyapatite/yttria stabilized zirconia composite coatings. J Am Ceram Soc 2002;85(4):800–6.

[14] Santos JD, Jha LJ, Monteiro FJ. In-vitro calcium phosphate formation on SiO_2–Na_2O–CaO–P_2O_5 glass reinforced hydroxyapatite composite: a study by XPS analysis. J Mater Sci: Mater Med 1996;7:181–5.

[15] Kokubo T, Kushitani H, Kitsugi S, Yamamuro T. Solutions able to reproduce in vivo surface structure changes in bioactive glass–ceramic A–W. J Biomed Mater Res 1990;24:721–34.

[16] Kweh SWK, Khor KA, Cheang P. An in vitro investigation of plasma sprayed hydroxyapatite (HA) coatings produced with flame-spheroidized feedstock. Biomaterials 2002;23(3):775–85.

[17] Kato R, Nakamura S, Katayama K, Yamashita K. Acceleration of bone-like crystal growth on polarized plasma sprayed HAp in SBF. Key Eng Mater 2002;218–2:145–8.

[18] Kokubo T. In: Yamamuro T, Hench LL, Wilson J, editors. Bonding mechanism of bioactive glass–ceramic A–W to living bone. CRC handbook of bioactive ceramics. Boca Raton, FL: CRC Press; 1990. p. 41–9.

[19] Leigh SH, Lin CK, Berndt CC. Elastic response of thermal spray deposits under indentation tests. J Am Ceram Soc 1997;80(8):2093–9.

[20] Anstis GR, Chantikul P, Lawn BR, Marshall DB. A critical evaluation of indentation techniques for measuring fracture toughness. J Am Ceram Soc 1981;64:533–8.

[21] Radin SR, Ducheyne P. Plasma spraying induced changes of calcium phosphate ceramic characteristics and the effect on in vitro stability. J Mater Sci: Mater Med 1992;3:33–42.

[22] Fazan F, Marquis PM. Dissolution behaviour of plasma sprayed hydroxyapatite coatings. J Mater Sci: Mater Med 2000;11:787–92.

[23] de Groot K, Klein CPAT, Wolke JGC, de Blieck-Hogervorst JMA. In: Yamamuro T, Hench LL, Wilson J, editors. Plasma sprayed coatings of calcium phosphate CRC handbook of bioactive ceramics, vol. II. Boston: CRC Press; 1990. p. 3–16.

[24] Gledhill HC, Turner IG, Doyle C. In vitro dissolution behavior of two morphologically different thermally sprayed hydroxyapatite coatings. Biomaterials 2001;22:695–700.

[25] Gross K, Berndt CC, Goldschlag DD, Iacono VJ. In vitro changes of hydroxyapatite coatings. Int J Oral Maxillofacial Implants 1997;12(5):589–97.

[26] Ning CQ, Zhou Y. In vitro bioactivity of a biocomposite fabricated from HA and Ti powders by powder metallurgy method. Biomaterials 2002;23(14):2909–15.

[27] Chang E, Chang WJ, Wang BC, Yang CY. Plasma spraying of zirconia-reinforced hydroxyapatite composite coatings on titanium, Part II. Dissolution behaviour in simulated body fluid and bonding degradation. J Mater Sci: Mater Med 1997;8:201–11.

[28] Ducheyne P, Radin S, King L. The effect of calcium-phophate ceramic composition and structure on invitro behaviour, 1. Dissolution. J Biomed Mater Res 1993;27:25–34.
[29] Uchida M, Kim HM, Kokubo T, Miyaji F, Nakamura T. Bone like apatite formation induced on zirconia gel in a simulated body fluid and its modified solutions. J Am Ceram Soc 2001; 84(9):2041–4.
[30] Nancollas GH. In: Mann S, Webb J, Williams RJP, editors. In vivo studies of calcium phosphate crystallization. Biomineralization. Weinhein, Germany: VHC Verlagsgesellschaft; 1989.